Design of a Permanent Magnet Wiggler for a THz Free Electron Laser

N. Balal*, E. Magori and A. Yahalom
Department of Electrical and Electronic Engineering, Faculty of Engineering, Ariel University, Ariel, Israel

(Received May 21, 2015)

A THz free electron laser is being built in Ariel University. Upon completion it is intended to become a user facility. The free electron laser is designed to emit radiation between 1 and 5 THz. It is planned to operate in the super radiance regime. The anticipated output of the free electron laser is in excess of 150 kW instantaneous power. An essential part of every free electron laser is a device generating a periodic magnetic field denoting the wiggler. Here we describe a design of a classical Halbach type permanent magnetic wiggler for the THz free electron laser. The main novelty in this paper is the choice of wiggler parameters suitable for operation in the THz frequency range. Considerations such as radiation wave length, wiggler gain and electron optics are taken into account.

DOI: 10.12693/APhysPolA.128.259
PACS: 03.50.–z, 07.55.Db, 07.57.Hm

1. Introduction

Over the past years, there has been a significant interest in employing terahertz (THz) technology, spectroscopy and imaging for security applications. There are three prime motivations for this interest:

1. THz radiation can detect concealed weapons since many non-metallic, non-polar materials are transparent to THz radiation (and are not transparent to visible radiation).

2. Target compounds such as explosives and illicit drugs have characteristic THz spectra that can be used to identify these compounds.

3. THz radiation poses no health risk for scanning of people (as opposed to X-rays).

Of course, millimeter wave (MMW) systems for detecting hidden weapons are quite common those days in airports and other public places. However, terahertz detection inherently has about ten times better spatial resolution compared to MMW systems simply because the electromagnetic wavelength of THz radiation is roughly ten times shorter than MMW radiation. Consequently, images of suspicious objects such as concealed metallic or plastic knives are much sharper and more readily identified when imaged with THz scanners. A smaller wavelength means a smaller antenna and therefore a shorter near field — and a closer far field which have beneficial implications for imaging.

A further important consideration is specificity. Through known characteristic THz spectra of explosives, biological and chemical agents and illegal drugs, a THz image can be spectroscopically analysed to identify concealed contents and potential threats. This capability is particularly important for explosives, for example, those have low vapour pressures and therefore would pose a challenge to trace vapour detection techniques. Many drugs and explosives have unique spectral lines in the THz regime which can facilitate their identification even when they are hidden and invisible to the naked eye. A list of such lines is given in Table.

TABLE

Unique spectral lines of explosives and drugs [1].

Material	Feature band center position frequency [THz]
Explosive	
Semtex-H	0.72, 1.29, 1.73, 1.88, 2.15, 2.45, 2.57
PE4	0.72, 1.29, 1.73, 1.94, 2.21, 2.48, 2.69
RDX/C4	0.72, 1.26, 1.73
TNT	5.6, 8.2, 9.1, 9.9
NH_4NO_3	4, 7
Drugs	
Methamphetamine	1.2, 1.7–1.8
MDMA	1.4, 1.8
Lactose α-monohydrate	0.54, 1.20, 1.38, 1.82, 2.54, 2.87, 3.29
Icing sugar	1.44, 1.61, 1.82, 2.24, 2.57, 2.84, 3.44
Co-codamol	1.85, 2.09, 2.93
Aspirin, soluble	1.38, 3.26
Aspirin, caplets	1.4, 2.24
Acetaminophen	6.5
Terfenadine	3.2
Naproxen sodium	5.2, 6.5

*corresponding author; e-mail: nezahb@ariel.ac.il

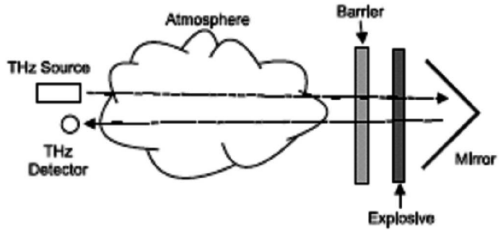

Fig. 1. Stand-off detection scheme [1].

Comparable spectroscopic "fingerprint" spectra of these threats are not present in the MMW range. In realistic situations the THz must pass several barriers before it reached a detector (see Fig. 1).

Hence both a high power source and a sensitive detector are required. A THz FEL is being built in Ariel University [2] to provide for a high power THz radiation source. This project is a collaboration between Ariel University, Tel Aviv University, and UCLA. Upon completion it is intended to become a user facility. The FEL is based on a compact photo cathode gun (60 cm) that will generate an electron beam at energies of 4.5–6.5 MeV. The pulses are planned to be of 300 pC for a single pulse, and of up to 1.5 nC for a train of pulses. The FEL is designed to emit radiation between 1 and 5 THz. It is planned to operate in the super radiance regime. The anticipated output of the FEL is in excess of 150 kW instantaneous power [2]. The bunching of the electron beam will be achieved by mixing two laser beams on the photocathode. The compression of the beam will be achieved by introducing an energy chirp to the beam and passing it through a helical chicane. We plan on compressing the single pulse to less than 150 fs. An essential part of every FEL is a device generating a periodic magnetic field denoted the wiggler. Here we describe a design of a planar Halbach [3] type permanent magnetic wiggler for the THz FEL. This type of wiggler (and its modifications) is quite popular in free electron lasers and as radiation sources in electron storage rings see for example [4–6]. We chose to adopt the classical design and thus the main novelty is the unique wavelength chosen and the super-radiant approach.

2. Halbach wiggler

The wiggler is a device consisting of a collection of magnets which are arranged in two rows in order to produce a periodic magnetic field [3] (see Fig. 2).

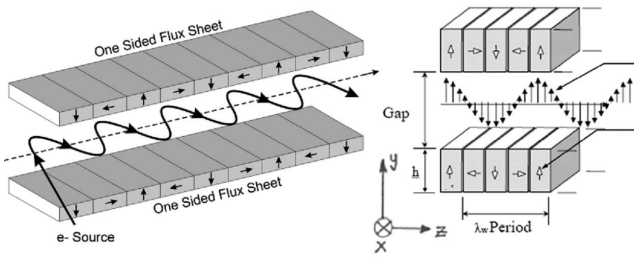

Fig. 2. Halbach planar wiggler.

Two magnetic lenses are used to focus the electron beam at the entrance and exit of the device. As the electron beam enters the wiggler, its periodic field causes the electrons to oscillate perpendicularly to the magnetic field. The wavelength of the oscillations is the same as that of the period of the wiggler. The wave length of the radiation emitted by the electrons is shorter due to the Doppler effect and the velocity of the accelerated electrons which typically move at the FEL with velocities about 99% of the speed of light. The wavelength of the radiation is given by the formula (1):

$$\lambda_{\mathrm{s}} = \frac{\lambda_{\mathrm{w}}}{\beta_z\left(1+\beta_z\right)\gamma_z^2} \approx \frac{\lambda_{\mathrm{w}}}{2\gamma_z^2}, \quad \beta_z = \frac{V_z}{c},$$
$$\gamma_z = \frac{1}{\sqrt{1-\beta_z^2}}, \quad \gamma = 1 + \frac{E_{\mathrm{k}}}{m_{\mathrm{e}}c^2}. \tag{1}$$

In the above λ_{s} is radiation wave length, λ_{w} is the wiggle cycle, V_z is the electrons velocity in the axial direction, c is the speed of light in vacuum, E_{k} is the kinetic energy of the electron and m_{e} is the electron mass. In the FEL scenario $\gamma \cong \gamma_z$. Halbach [1] has analyzed the magnetic field produced by his wiggler assuming it is infinite and obtained equation

$$B_y(y=0,z) = \tag{2}$$
$$2B_{\mathrm{r}}\frac{\sqrt{2}/2}{\pi/4}\,\mathrm{e}^{-\pi\frac{gap}{\lambda_{\mathrm{w}}}}\left(1-\mathrm{e}^{-2\pi\frac{h}{\lambda_{\mathrm{w}}}}\right)\cos\left(2\pi\frac{z}{\lambda_{\mathrm{w}}}\right),$$

in which only the dominant ($n = 1$) harmony is taken into account. The field depends on the magnet thickness (h), the distance between the jaws (gap), period length (λ_{w}) and the residual magnetic field of a single magnetic block (B_{r}). In the above the axis of the wiggler is the z axis. Magnetic field of the wiggler as a function of the height h for a gap of 0.871 cm and a period of 2 cm is shown in Fig. 3. The gap is determined by the size of waveguides in which the radiation and electrons travel plus an interval of 100 μm on each side. The residual magnetic field of the block magnets used is 1.1 T typical of $Nd_2Fe_{14}B$ or $SmCo_5$ magnets.

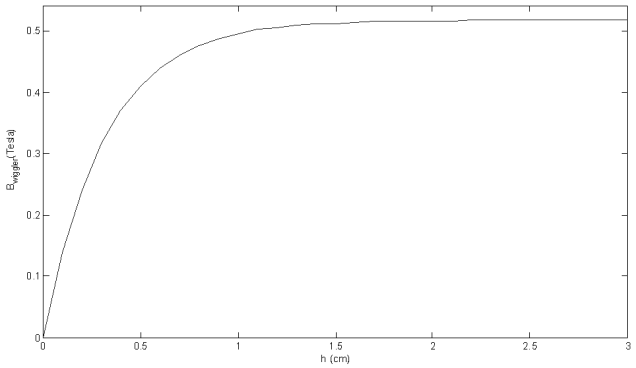

Fig. 3. The magnetic field in the middle of the wiggler as a function of the height of the magnet h. In the above B_{wiggler} is the maximal B_y field of Eq. (2) on axis.

According to Fig. 3 it can be seen that when the magnet height is greater than 1 cm the field saturates and therefore we have chosen to a height of 1.5 cm which yields a field of about 0.5 T. The field strength controls the amplitude of the electron oscillations and hence the amount of power generated by the oscillating electrons.

By Halbach's formula (2) we have found in the magnetic field dependence on the gap accuracy

$$\frac{\Delta B_y}{B_y} = -\frac{\pi}{\lambda_{\mathrm{w}}}\Delta gap. \tag{3}$$

For a period of $\lambda_{\mathrm{w}} = 20$ mm we obtain that a change in the gap of 60 μm causes a field change of one percent. As a result, the resolution of the gap sliding will be set to about 60 μm.

3. A finite Halbach wiggler

As seen above, the Halbach formula assumes an infinite width so it is necessary to examine what level of influence the width of the magnet has on the field. For this purpose, analytical formulae can be used for the three-dimensional field of a bar magnet [7]. The dimensions of a box magnet are: $(2x_{\mathrm{b}}, 2y_{\mathrm{b}}, 2z_{\mathrm{b}})$. The magnetization is directed in the y direction and magnetization magnitude is M_0. The formulae are

$$H_x(x,y,z) = \frac{M_0}{4\pi}\sum_{k,l,m=1}^{2}(-1)^{k+l+m}\ln\left(z+(-1)^m z_b+\sqrt{(x+(-1)^k x_b)^2+(y+(-1)^l y_b)^2+(z+(-1)^m z_b)^2}\right),$$

$$H_y(x,y,z) = -\frac{M_0}{4\pi}\sum_{k,l,m=1}^{2}(-1)^{k+l+m}\frac{[y+(-1)^l y_b][x+(-1)^k x_b]}{|y+(-1)^l y_b|\,|x+(-1)^k x_b|}$$

$$\times\arctan\left(\frac{\left|x+(-1)^k x_b\right|(z\ +(-1)^m z_b)}{\left|y+(-1)^l y_b\right|\sqrt{(x+(-1)^k x_b)^2+(y+(-1)^l y_b)^2+(z+(-1)^m z_b)^2}}\right),$$

$$H_x(x,y,z) = \frac{M_0}{4\pi}\sum_{k,l,m=1}^{2}(-1)^{k+l+m}\ln\left(x+(-1)^k x_b\ +\sqrt{(x+(-1)^k x_b)^2+(y+(-1)^l y_b)^2+(z+(-1)^m z_b)^2}\right). \tag{4}$$

A depiction of the magnet is given in Fig. 4.

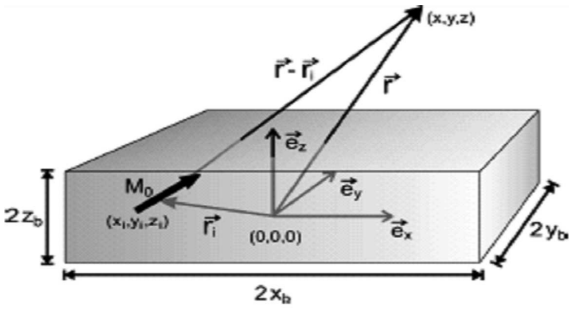

Fig. 4. Geometric description of the bar magnet [7].

A MATLAB calculation of 40 Halbach periods of square magnets done according to the above formulae yielded Fig. 5. It is obvious that on the magnetic axis the field has a periodicity of 2 cm and amplitude of the field is 0.5 T consistent with the result of Halbach (Eq. (2)) regarding the field strength shown in Fig. 3.

Analysis of the effect of the magnet width ($W = 2x_{\mathrm{b}}$) on the magnetic field magnitude is described in Fig. 6. It can be seen that if the width of the magnet is 30 mm or more the magnitude of the magnetic field does not depend on the width of the magnet for all relevant gaps.

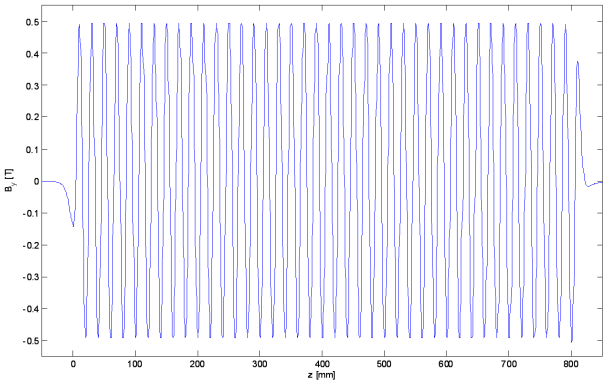

Fig. 5. Magnetic field along the z axis in the y direction resulting from 40 Halbach magnets described by the analytic expression (4).

According to Halbach's formula B_y is constant in the x axis. In reality the finite width of the magnet causes a decrease in B_y along the x axis (Fig. 7). As a result the electron beam is diverging in the x–z plane. Moreover, the beam spatial charge strengthens the divergence. This is seen in Fig. 8 describing GPT simulation results for beam transport. We assumed a charge of 300 pC, radius of 1.5 mm, pulse length of 300 fs and energy of 6 MeV.

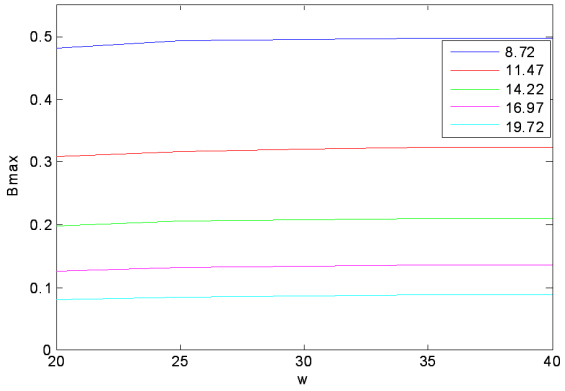

Fig. 6. The maximal size of the magnetic field ($B_{\max}$) along the axis depending on the width of the magnet (w) (for dimension in the x direction see Fig. 2) for different gaps.

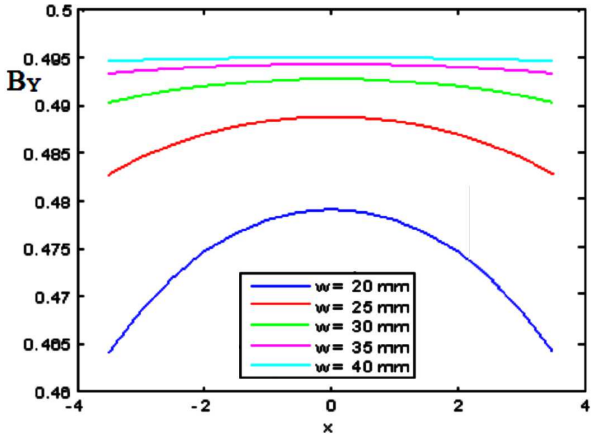

Fig. 7. B_y as a function of x for various magnet widths (see Fig. 2 for a definition of the x direction).

The simulation takes into account the effect of spatial charge. It can be seen that there is a collision of the beam with the waveguide walls (Fig. 8). Trajectories of particles hitting the walls of the waveguides are depicted as straight lines. Therefore for a good transport it is necessary to introduce a centering device such as a pair of long magnets as in Fig. 9.

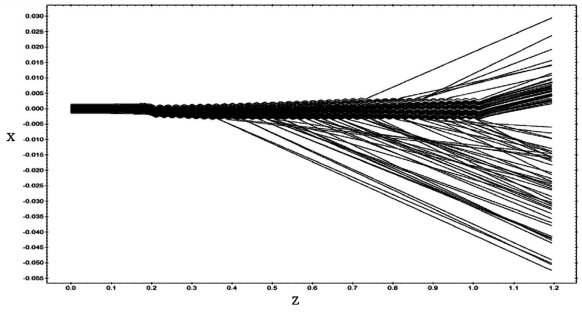

Fig. 8. Electron trajectories within a wiggler in the absence of a centering device.

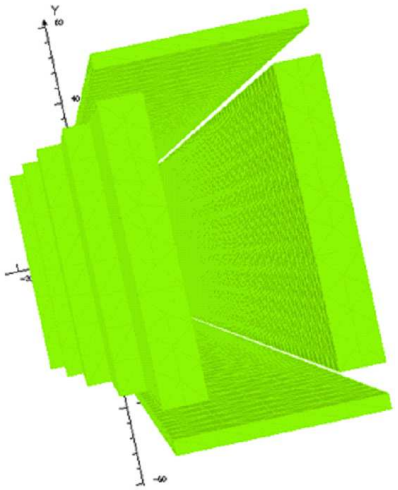

Fig. 9. Two long magnets serving as a centering device. Those magnets correct the diverging electron trajectories seen in Fig. 8.

For mechanical design of the wiggler one needs to know in advance the force acting between the two "jaws" of the magnets which is calculated according to

$$F_{\mathrm{M}} = \frac{1}{2\mu_0} \int \int B_y^2 \left(x, y = 0, z\right) \mathrm{d}x \mathrm{d}z. \tag{5}$$

For a maximum intensity on the axis equal to 0.5 T, wiggler length (L) of 0.8 m and width of (W) 0.03 m we obtain

$$F_{\mathrm{M}} = \frac{B^2 W L}{4\mu_0} = 1.2 \text{ kN}. \tag{6}$$

The maximum opening of the gap is defined by the requirement of force between the jaws of one kilogram. Looking at Fig. 10 it is easy to see that this requires a maximum gap of 25 mm in which the magnetic field is less than 0.05 T.

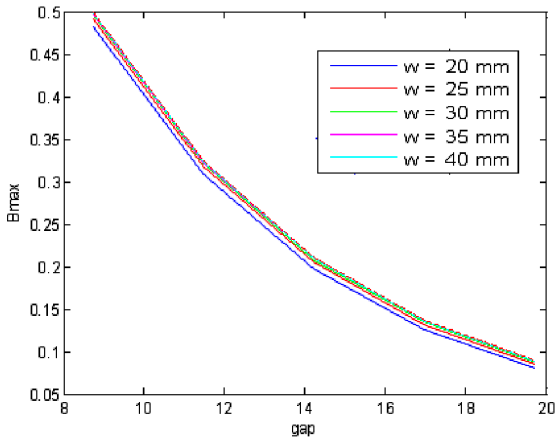

Fig. 10. Maximum magnetic field as function of the gap between the magnets, the different coloured lines stand for different widths. The dashed line is the "infinite" width case which is described by Halbach formula (2).

4. Conclusion

We have reported some details regarding the wiggler for the THz FEL designed in Ariel University. In particular we have calculated the period length, the height and the width of the magnets. We have also suggested correction side magnets to correct for diverging electron trajectories and also calculated the forces between the jaws of the wiggler magnets to facilitate a mechanical design. More details that cannot fit in an eight pages paper will be given hopefully in a future (longer) paper. The components of the wiggler have been ordered according to the design specified above and we hope to be able to report the results of the measurements soon. The calculations of the THz radiation power generated by our FEL can be found in [2]. The FEL is expected to be operative in about two years.

References

[1] C. Michael, P. Kemp, F. Taday, B.E. Cole, J.A. Cluff, A.J. Fitzgerald, W.R. Tribe, *Proc. SPIE* **5070**, 44 (2003).

[2] A. Friedman, N. Balal, E. Dyunin, Y. Lurie, E. Magori, V.L. Bratman, J. Rosenzweig, A. Gover, in: *36th Int. Free Electron Laser Conf. FEL2014*, Basel 2014, TUP081.

[3] K. Halbach, *Nucl. Instrum. Methods* **169**, 1 (1980).

[4] G. Brown, K. Halbach, J. Harris, H. Winick, *Nucl. Instrum. Methods Phys. Res.* **208**, 65 (1983).

[5] M.R. Asakawa, N. Inoue, K. Mima, S. Nakai, K. Imasaki, M. Fujita, *Nucl. Instrum. Methods Phys. Res. A* **358**, 399 (1995).

[6] G. Isoyama, M. Fujimoto, R. Kato, S. Yamamoto, K. Tsuchiya, *Nucl. Instrum. Methods Phys. Res. A* **507**, 234 (2003).

[7] R. Engel-Herbert, T. Hesjedal, *J. Appl. Phys.* **97**, 074504 (2005).